Tomasz Kozior,[1] Nonsikelelo Sheron Mpofu,[2,3] Johannes Fiedler,[2] Andrea Ehrmann[2]
[1] Faculty of Mechatronics and Mechanical Engineering, Kielce University of Technology, 25-314 Kielce, Poland
[2] Faculty of Engineering and Mathematics, Bielefeld University of Applied Sciences and Arts, Bielefeld, Germany
[3] School of Engineering, Moi University, Eldoret, Kenya

Influence of Textile Substrates on the Adhesion of PJM-Printed MED610 and Surface Morphology

Vpliv tekstilnega substrata na adhezijo smole MED610, natisnjene s tehniko kapljičnega nanašanja PJM, in morfologija površine

***Original scientific article**/Izvirni znanstveni članek*
Received/*Prispelo* 6–2024 • Accepted/*Sprejeto* 8–2024

Corresponding author/*Korespondenčni avtor:*
Tomasz Kozior
E-mail: tkozior@tu.kielce.pl
ORCID iD: 0000-0002-8922-4187

Abstract

The idea of 3D printing on textile fabrics was first mentioned around 10 years ago and has been investigated in detail since. Originally aimed at opening new design possibilities, combining 3D printing with textile substrates has shifted towards a new method to prepare composites with defined mechanical and other physical properties. The main problem of fused deposition modelling (FDM; also referred to as material extrusion (MEX) according to ISO/ASTM 52900) is printing on textile fabrics, where the frequently insufficient adhesion between both materials has not been fully resolved. For this reason, a few attempts have been made to combine other additive manufacturing methods with textile fabrics. While the principle possibility of using stereolithography (SLA) on textile fabrics was demonstrated a few years ago, PolyJet modelling (PJM) has only recently proven to be applicable for direct printing on textile materials. Here, we present the first study of printing MED610 medical resin on different fabrics. We show that a higher textile fabric surface roughness generally increases the adhesion of the printed material, while a higher hydrophobicity is disadvantageous. We also tested the influence of textile substrates on the porosity of the MED610 surface, as this parameter can influence a material's potential use in tissue engineering and other biomedical applications.
Keywords: material extrusion, MEX, adhesion, fused deposition modelling, FDM

Izvleček

Ideja o 3-D tiskanju na tekstil je bila prvič omenjena pred približno desetimi leti in je bila od takrat podrobno raziskana. Kombinacija 3-D tiskanja s tekstilnimi materiali, ki je bila prvotno namenjena odpiranju novih možnosti oblikovanja, se je pozneje preusmerila na nove metode za pripravo kompozitov z definiranimi mehanskimi in drugimi fizikalnimi lastnostmi. Glavna težava modeliranja taljenega nanašanja (FDM; imenovana tudi ekstruzija materiala (MEX) v skladu z ISO/ASTM 52900) je tiskanje na tekstilije, kjer pomanjkljivost nezadostne adhezije med obema materialoma

še ni bila v celoti odpravljena. Zato je bilo narejenih nekaj poskusov kombiniranja drugih metod aditivne tehnologije s tekstilijami. Medtem ko je bila glavna možnost uporabe stereolitografije (SLA) na tekstilijah prikazana pred nekaj leti, se je modeliranje PolyJet (PJM) izkazalo za uporabno za neposredno tiskanje na tekstilne materiale šele pred kratkim. V tem članku je predstavljena prva študija tiskanja medicinske smole MED610 na različne tkanine. Dokazano je, da na povečanje adhezije natisnjenega materiala vpliva večja površinska hrapavost tekstilije, medtem ko večja hidrofobnost to adhezijo poslabša. Preizkušen je bil tudi vpliv tekstilnih materialov na poroznost površine MED610, saj lahko ta parameter vpliva na potencialno uporabo materiala v tkivnem inženirstvu in drugih biomedicinskih aplikacijah.
Ključne besede: ekstrudiranje materiala, MEX, adhezija, modeliranje taljenega nanosa, FDM

1 Introduction

In the last decade, additive manufacturing has developed further from a tool for rapid prototyping towards the possibility of the rapid production of unique parts that frequently could not be produced using other techniques. The fused deposition modelling FDM (or material extrusion, MEX) printing process is used most, and is based on inexpensive machines and polymer materials [1]. Stereolithography (SLA), the very first 3D printing technique, is also widely used today [2]. There are, however, many more additive manufacturing techniques available, which facilitate the printing of diverse polymers, metal and various blends with different accuracies [3–5].

Representing one of the main problems of 3D printed objects, in addition to frequently insufficient dimensional accuracy, are mechanical properties, which are often diminished in comparison with injection moulded objects due to the layer-wise build-up [6, 7]. Different possibilities have been suggested to improve tensile and bending properties, such as thermal post-treatment [8,9], the integration of fibrous or other fillers in the printed polymer [10, 11] or the optimization of printing parameters [12, 13]. A completely different approach is given by combining 3D printing, especially FDM printing, with a textile fabric to form a composite with improved lateral mechanical properties.

In this approach, the main problem is the adhesion between the textile substrate and the imprinted polymer [14–16]. This topic has been investigated in detail by several research groups in the last decade, revealing several parameters that influence adhesion in the case of FDM printing on textile fabrics, such as extrusion temperature and printing speed [17], the surface structure of the fabrics, as well as the mass per unit area and thickness thereof [18–20]. While a thermal after-treatment of the composite was only found to have a positive impact in some experiments [21, 22], the chemical pretreatment of the textile fabric to reduce hydrophobicity was reported to be advantageous in many cases [22–24]. Most importantly, the z-distance between nozzle and fabric must be tailored carefully to press the FDM polymer sufficiently deep into the textile fabric to reach a form-locking connection, while avoiding the clogging of the nozzle [25, 26].

The latter point is different when SLA or other resin-based 3D printing techniques are applied to print on textile fabrics. On the one hand, SLA resins are significantly less viscous than the molten polymers used in FDM printing, making it easier for them to penetrate through the fabric and build a form-locking connection [27]. On the other hand, pressing the resin into the fabric is usually not possible in resin-based printing processes.

While the possibility of performing SLA printing on textile fabrics was already reported in 2020, PolyJet modelling (PJM) on textile fabrics was only shown recently for the first time [28]. This method has the advantage of not inserting the whole fabric into the resin, as is necessary in SLA printing; instead the resin is only placed at the desired positions [28].

Here, we extended the first proof-of-principle of PJM printing on textiles by using another resin,

MED610, which is mainly used in medicine and dentistry [29], to increase the potential range of applications and avoid potentially toxic materials. Different woven fabrics are tested to investigate the influence of textile surface roughness on adhesion, and to test whether the Korger rule [30], stating that hydrophilic textiles enable a higher adhesion than hydrophobic ones, also holds true for PJM printing. Finally, the potential influence of a textile substrate on the surface porosity of the MED610 surface was investigated, as this parameter plays an important role in tissue engineering and other biomedical applications in which MED610/textile composites may be used [31–33].

2 Materials and methods

Two different sets of textiles were tested in this study. The first set consisted of three woven fabrics from cotton (thickness 0.34 mm, mass per unit area 143 g/m²), linen (0.54 mm, 196 g/m²), and polyester (PES) "micropeach", which is roughened on one side (0.38 mm, 127 g/m²). All three textiles were also investigated in [28] and were found suitable for PJM printing using Fullcure720 PJM resin. The second set of samples contained PES woven fabrics in plain weave (thickness 0.32 mm, mass per unit area 167 g/m²), twill weave 2/1 (0.32 mm, 186 g/m²), and Leno (0.48 mm, 181 g/m²). These three samples were recently investigated in terms of FDM and SLA printing [34], and thus allow for a direct comparison of two resin-based printing methods, although with different resins according to the limited availability of materials for both printing methods.

3D printing was performed with the aforementioned MED610 medical resin (Stratasys, Eden Prairie, MN, USA), certified as biocompatible material according to ISO 10993-1:2009 [35,36]. A Connex 350 PJM printer (Stratasys) was used to prepare rectangular samples ($n = 3$) for adhesion tests according to DIN 53530, which were evaluated according to DIN ISO 6133. These adhesion tests were performed using a Sauter FH2K universal test machine. Confocal laser scanning microscope (CLSM) images were taken using a VK-8710 (Keyence, Neu-Isenburg, Germany) and evaluated using ImageJ 1.53e software (National Institutes of Health, Bethesda, MD, USA). Water contact angles were measured at a magnification of 5x using a USB microscope.

3 Results and discussion

While the water contact angle of the front side of the PES "micropeach" fabric (on which printing was performed) was measured as (123 ± 6)°, all other materials were highly hydrophilic, with water drops spreading very fast in the other three (untreated) PES fabrics and the linen fabric, and spreading slower in the cotton fabric. According to the Korger rule, this leads to the first assumption that the adhesion should be highest on linen and the untreated PES fabrics and lowest on the PES "micropeach" [22, 23].

Indeed, the adhesion tests revealed the highest adhesion forces for MED610 on linen, as the exemplary measurement curves in Figure 1a show. Here it can also be seen that the curve measured for MED610 on linen varies more than the others, while the adhesion on PES micropeach varies only slightly. This can be attributed to the different surface morphologies, as will be discussed later.

This means that different evaluation methods according to ISO 6133 must be used for cotton, linen and Leno on the one hand (procedure C, for graphs with more than 20 peaks) and for the PES micropeach, PES plain weave and twill on the other hand (procedure D, for wavy curves). This must be taken into account in the discussion of adhesion values.

Interestingly, the adhesion values of MED610 on plain weave and twill are relatively low (Figure 1b), while the values on the thicker Leno fabric are similar to those found on the cotton fabric. The adhesion on the Leno fabric was even high enough to destroy two of the three fabrics during the adhesion tests. Here, apparently not the hydrophobicity, but

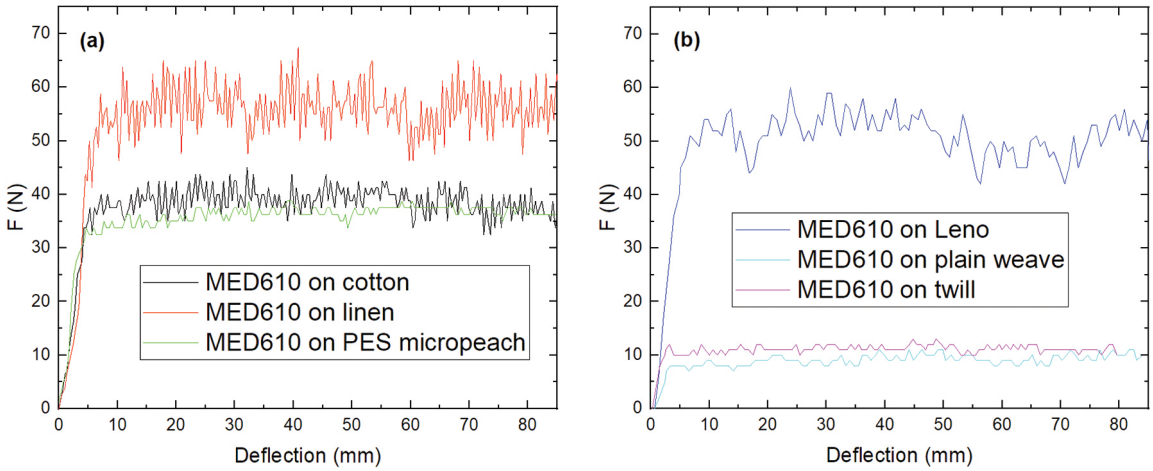

Figure 1: Exemplary adhesion test curves of MED610 on (a) cotton, linen and PES micropeach, (b) polyester plain weave, twill weave and Leno fabric.

the thickness of the fabric plays an important role, as both the thickest fabrics (linen and PES Leno) show clearly higher adhesion than the other woven fabrics. The low adhesion values of the PES plain weave and twill weave fabrics, on the other hand, can be explained by their dense woven structure without large air voids, as can be seen by comparing their apparent densities (calculated as the mass per fabric volume) or the corresponding porosities (calculated from a comparison of the apparent density with the respective material's bulk density, using literature values of 1.5 g/cm³ for PES, 1.51 g/cm³ for cotton and 1.4 g/cm³ for linen).

Table 1 gives an overview of the parameters that can initially be deemed to have an influence on adhesion, with the colours ranging from green (positive impacts) to red (negative impacts). According to this table, both PES plain and twill weave should show the lowest adhesion, followed by PES micropeach and cotton, while linen and the Leno fabric should have the highest adhesion. This corresponds to the findings of Figure 1.

Table 1: Colour-coded influence of different parameters on the adhesion on the tested woven fabrics

Sample	Hydrophobicity	Thickness (mm)	Apparent density (kg/m³)	Porosity (%)
PES "micropeach"	Hydrophobic	0.38	334	78
Cotton	Hydrophilic	0.34	421	72
Linen	Hydrophilic	0.54	363	74
PES plain weave	Hydrophilic	0.32	522	65
PES twill 2/1	Hydrophilic	0.32	581	61
PES Leno	Hydrophilic	0.48	377	75

The evaluation of the adhesion tests and a comparison with previous tests on the same materials are shown in Figure 2. First, when comparing the adhesion values for MED610 on the different woven fabrics, it is obvious that the adhesion on linen is highest, as expected from Figure 1, followed by PES Leno. Comparing the adhesion of MED610 on cotton and PES micropeach, the calculated value for the latter is significantly lower according to Figure 2, while both were similar in Figure 1. This can be explained by the aforementioned different evaluation methods, leading to the average of all adhesion values of PES micropeach, while only peaks were counted for cotton and linen.

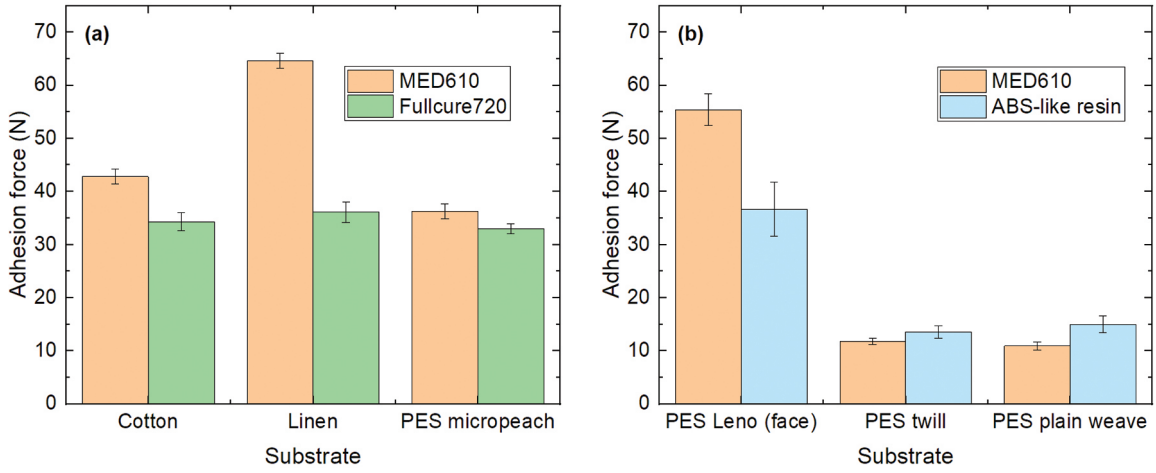

Figure 2: (a) Comparison of the adhesion of MED610 (new values) and Fullcure720 (values from [28]) on cotton, linen and PES micropeach; (b) comparison of the adhesion of MED610 printed with PJM (new values) with the adhesion of "ABS-like resin" printed using SLA (values from [31]).

Most interestingly, especially for linen, the adhesion could be significantly increased compared to the previous measurement with Fullcure720 [28]. While both resins have a similar viscosity and can thus be expected to flow into the textile materials in a similar way, the recent printing processes were performed by carefully calculating the z-position of the first printed layer according to the textile thickness. It can thus be speculated that optimizing the z-position of the PJM printed material can also be used to improve the adhesion on a textile fabric, similar to the necessary optimization of the z-distance between nozzle and printing bed for FDM printing on textile fabrics [25, 26]. While this optimization process was not developed further in this study, it will be investigated further in the near future.

Comparing the resin-based methods FDM and SLA printing (Figure 2b), the values for the thinner fabrics are quite similar, while the Leno fabric revealed a higher adhesion for PJM, indicating that this technique may be advantageous for thicker fabrics. However, a larger study comparing these techniques is necessary to reveal all their advantages and disadvantages.

Besides the hydrophobic/hydrophilic properties of textile substrates, their thickness and apparent density (cf. Table 1), their surface structure can also be expected to influence adhesion. Figure 3 depicts CLSM images of the back of the MED610 printed material after the adhesion tests on the first set of samples, showing the surface morphology (left panels) as well as the colour-coded heights (right panel). For all three textile fabrics, the woven structure is clearly visible, showing how precisely the low-viscous resin follows the textile surface during printing. This is a clear advantage of PJM printing over FDM printing. In addition, there are differences visible between cotton (showing a few protruding fibres, visible as red-orange colours), linen (showing many more fibres), and PES micropeach (without fibres). A larger number of fibres can also be expected to support adhesion, as would be the case for FDM printing.

After the investigation of the adhesion between MED610 and the different fabrics, the potential influence of the textile substrates on the MED610 surface was examined for the first set of samples. This is especially important for this resin due to its potential use in biomedical applications, where the growth of mammalian cells, for example, is strongly influenced by surface porosity. An initial comparison of the surfaces of MED610 printed purely on the printing bed and printed on the different textiles, respectively, is shown in Figure 4. Nine more images of each set of samples are shown in the appendix.

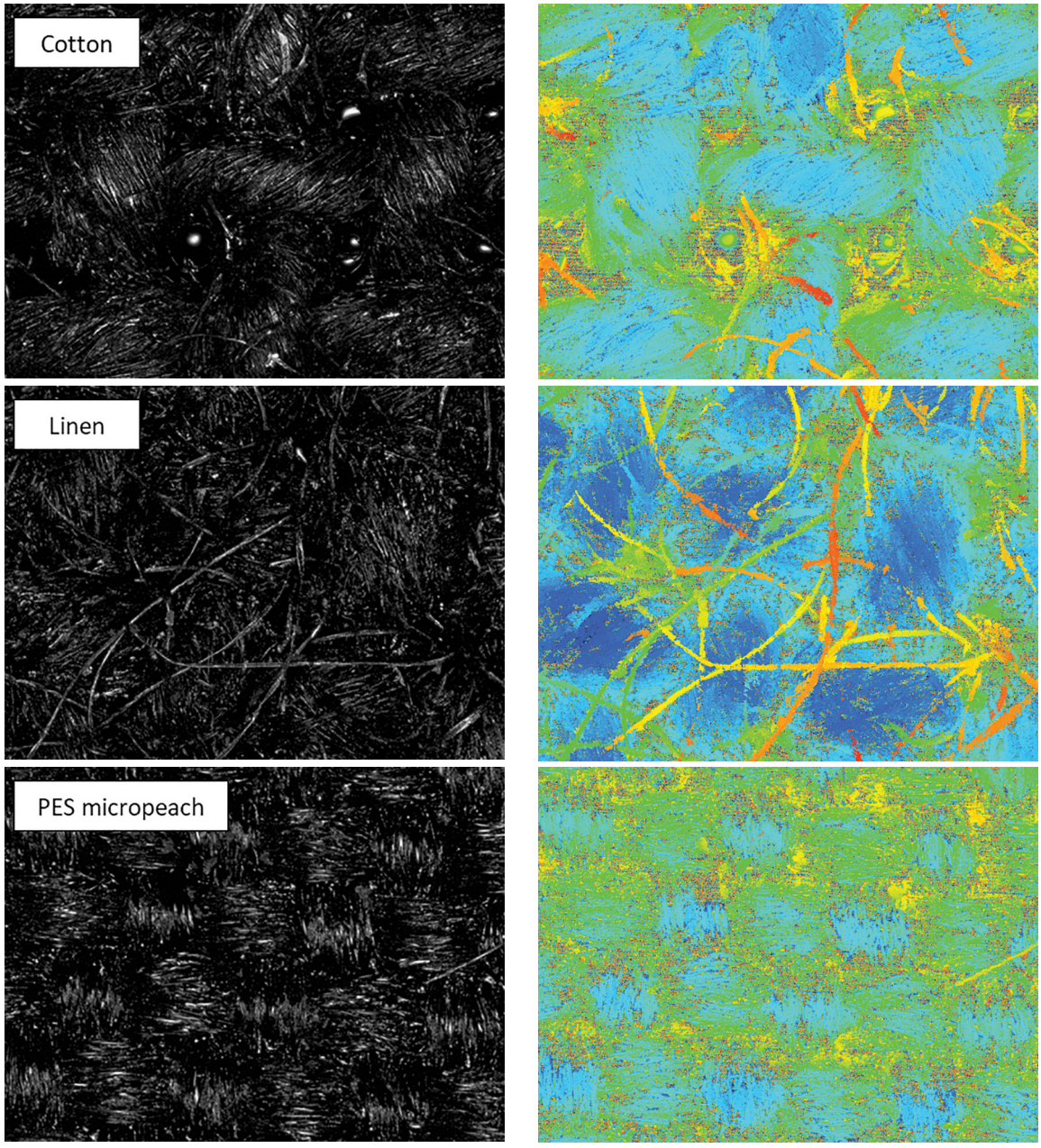

Figure 3: CLSM images on the back of MED610 detached from different textile fabrics, showing the optical appearance (left panels) and the heights (right panels). In the latter, blue shows the lowest areas and red the highest areas. Images sizes correspond to 1.4 mm × 1.05 mm.

The first optical impression of these images is that there are more "large" holes visible on the surface of the pure MED610, while printing on textile fabrics leads to more small holes. However, this first impression should be quantified, taking into account a larger number of CLSM images. For this reason, additional images at three positions of each of the three samples were taken (cf. appendix). Next, a procedure had to be defined to quantitatively evaluate the numbers of small and large holes in these images.

Used for this purpose was the ImageJ software, which can count particles in an image. The following process was followed to set the colour threshold and to count the particles:

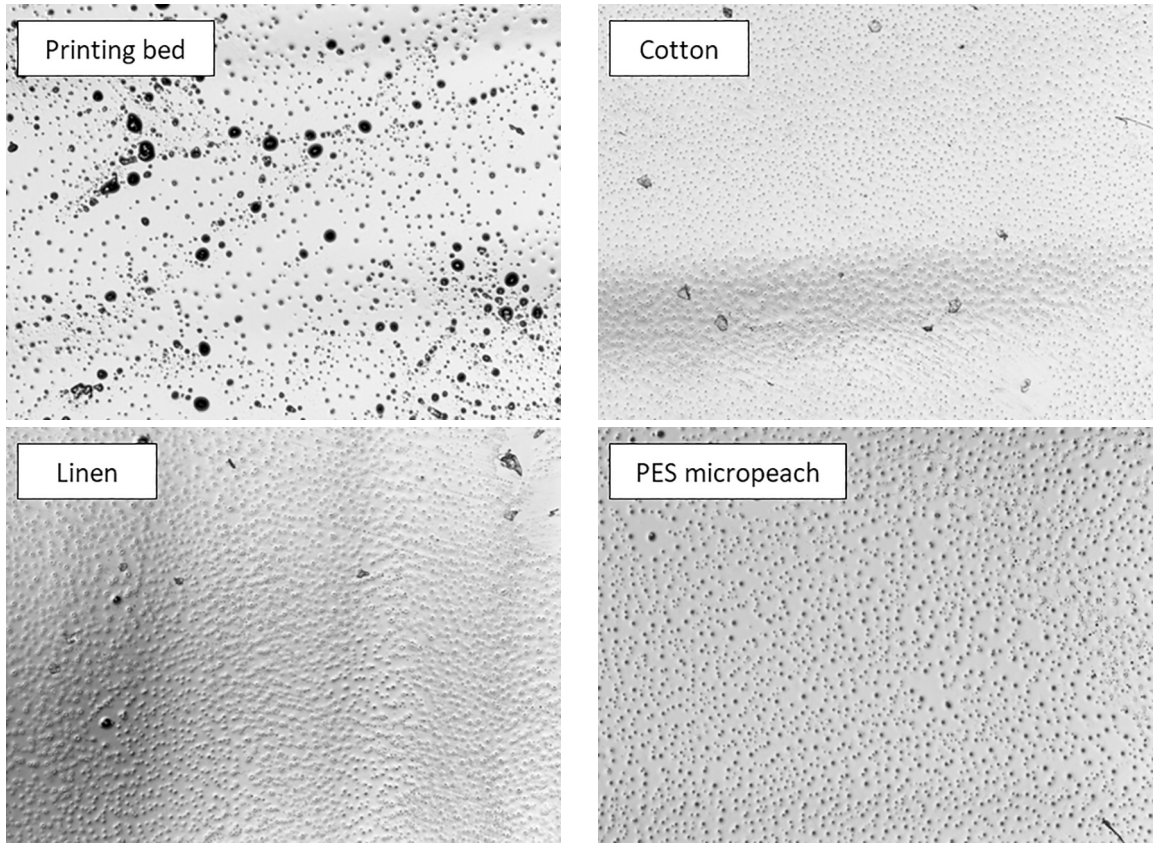

Figure 4: CLSM images of the surfaces of MED610 printed on the usual printing bed and different textile fabrics, respectively. Images sizes correspond to 1.4 mm × 1.05 mm.

- Image → Adjust → Colour threshold
- Analyse→ Analyse particles

The following definitions were chosen for this paper:

- A threshold area of 400 pixels was chosen for "small" holes. The image size of 2048 x 1536 pixels corresponds to 1.4 mm x 1.05 mm, so that a 400-pixel area (i.e. a hole diameter of 22.5 pixels) corresponds to 15.4 µm. This value was chosen as typical mammalian cells have diameters of around 10 µm, so that a slightly larger hole size may be supportive for mammalian cell adhesion and proliferation.
- The "larger" holes were further subdivided into "irregular" (circularity 0.00-0.07) and "round" holes (circularity 0.71-1.00), where the cut-off for the circularity was subjectively chosen. All "large" holes were manually checked to avoid misinterpretations due to an inappropriate colour threshold.

It should be mentioned that these values can naturally be chosen in any other way; these values were used as a first approach to quantify the apparent optical differences between different surfaces. The results are presented in Figure 5.

Generally, Figure 5 shows a slight tendency towards smaller numbers of small and large holes on linen, and larger numbers on pure MED610, but no significant differences are visible, as the very large error bars show. An optical investigation of the CLSM images in the appendix reveals a similar finding: large differences occur between different samples of the same material combinations, e.g. comparing samples S1 and S2 in Figure A2 with

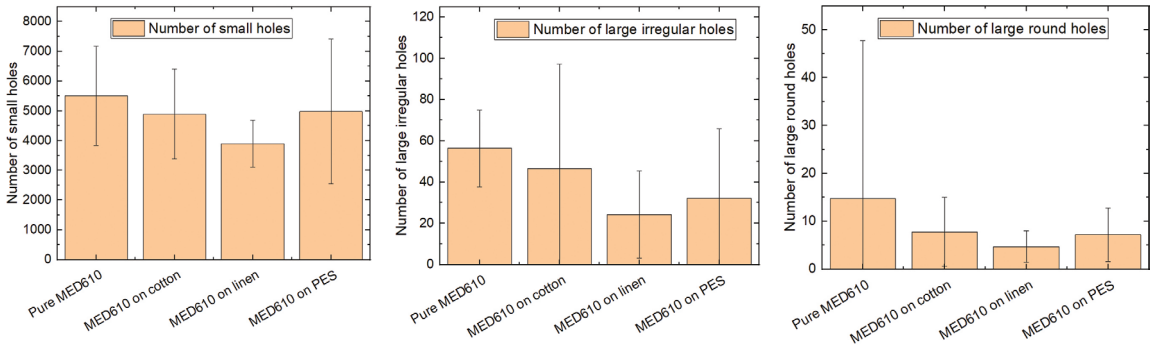

Figure 5: Numbers of small, large irregular, and large round holes on MED610 surfaces, counted with the above described process on ten CLSM images per material combination.

sample S3, and even comparing different positions on one sample, e.g. positions P2 and P3 of sample S1 in Figure A4. On the other hand, the optically most homogeneous surface with the fewest large holes can all be found for MED610 printed on cotton or linen fabrics (Figure A2, A3), suggesting that the potential influence of printing on textile fabrics on the MED610 surface should be investigated further, although the quantitative analysis of the holes in the surface did not reveal significant differences.

Finally, it should be mentioned that the chosen method here, applying an automatic cut-off value for brightness in order to separate holes from the surrounding area, shows very different stability against variations of this cut-off value for different images. As an example, Figure 6 shows for two images on the same MED610 sample on cotton (cf. Figure A2), taken on different spots of the sample surface (positions P1 and P2 on sample S1), the numbers of small holes counted for different brightness cut-offs. While for position P1 (black dots), the automatically set brightness cut-off value leads to a number of small holes near the maximum that can be reached by varying the cut-off value, this is completely different for position P2 on the same sample (red dots). As these examples show, the brightness cut-off value can strongly influence the number of counted small holes, making this value highly unreliable. This investigation was thus not repeated for the second set of samples.

The results showed that a pragmatic evaluation based on a threshold value does not lead to stable

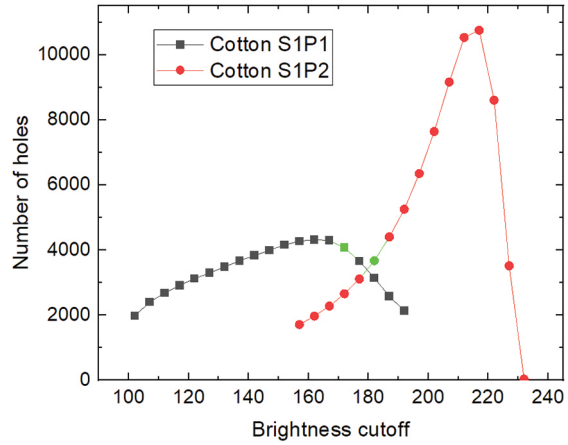

Figure 6: Numbers of small holes on MED610 on cotton, counted on two positions of the same sample (cf. Figure A2), depending on the brightness cut-off. The green dots correspond to the automatically set brightness cut-off values.

and reliable statements. For further investigations, other image evaluation algorithms should be used for a reliable analysis of the image data. For image data that has overall homogeneous grey value data, the threshold value could be adjusted by evaluating the histogram data of an image. If the grey values within an image fluctuate considerably, gradient filters or other approaches from image preprocessing could be used. The use of neural networks for object detection, such as the Segment Anything Model (SAM) from Meta AI, should also be considered. Further investigations of the image data should follow from this.

4 Conclusion and outlook

MED610 medical resin was PJM-printed on different textile fabrics. The highest adhesion values were found for the most hydrophilic and hairy linen woven fabric, as expected, directly followed by a PES Leno fabric with similarly low apparent density and relatively high fabric thickness. For the first set of samples, adhesion could be increased compared to a previous study using Fullcure720 [28], which can be attributed to the better setting of the first layer z-position. For the second set of samples, similar values were found as in a previous study on SLA printing on these materials [31]. In addition, CLSM images revealed a tendency towards a more homogeneous surface with fewer large holes when printing especially on linen woven fabric, which may support the use of MED610 in tissue engineering and other potential applications.

Generally, a good adhesion could be correlated with relatively thick, hydrophilic fabrics with a low apparent density. Both the dependence of adhesion on the setting for the first layer z-position and the influence of different substrates on the surface morphology will be further investigated in a subsequent study aimed at providing reliable rules for optimized PJM printing on textile fabrics.

Acknowledgment

This article was written during the research stay of Nonsikelelo Sheron Mpofu at Bielefeld University of Applied Sciences and Arts (HSBI). The research stay was funded through the New Horizons Fellowship from HSBI's Central Gender and Diversity Officer. The authors would like to thank Alexander Büsgen and Thomas Berger from Niederrhein University of Applied Sciences (Germany) for the woven polyester fabrics (second set of samples).

References

1. SCHMELZLE, John, KLINE, Eric V., DICKMAN, Corey J., REUTZEL, Edward W., JONES, Griffin, SIMPSON, Timothy W. (Re)designing for part consolidation: understanding the challenges of metal additive manufacturing. *Journal of Mechanical Design,* 2015, **137**(11), 1–12, doi: 10.1115/1.4031156.
2. NOORANI, Rafiq. *Rapid Prototyping: Principles and Applications*. Hoboken : Wiley, 2005.
3. CHEN, Qian, LIU, Jikai, LIANG, Xuan, TO, Albert C. A level-set based continuous scanning path optimization method for reducing residual stress and deformation in metal additive manufacturing. *Computer Methods in Applied Mechanics and Engineering,* 2020, **360**, 1–29, doi: 10.1016/j.cma.2019.112719.
4. NEUMANN, Taylor V., DICKEY, Michael D. Liquid metal direct write and 3D printing: a review. *Advanced Materials Technologies*, 2020, **5**(9), 1–16, doi: 10.1002/admt.202000070.
5. HADA, Tamaki, KANAZAWA, Manabu, IWAKI, Maiko, ARAKIDA, Toshio, SOEDA, Yumika, KATHEN, Awutsadaporn, OTAKE, Ryosuke, MINAKUCHI, Shunsuke. Effect of printing direction on the accuracy of 3D-printed dentures using stereolithography technology. *Materials*, 2020, **13**(15), 1–12, doi: 10.3390/ma13153405.
6. CARPENTER, Kevin, TABEI, Ali. On residual stress development, prevention, and compensation in metal additive manufacturing. *Materials,* 2020, **13**(2), 1–38, doi: 10.3390/ma13020255.
7. GENDVILIENE, Ieva, SIMOLIUNAS, Egidijus, REKSTYTE, Sima, MALINAUSKAS, Mangirdas, ZALECKAS, Linas, JEGELEVICIUS, Darius, BUKELSKIENE, Virginija, RUTKUNAS, Vygandas. Assessment of the morphology and dimensional accuracy of 3D printed PLA and PLA/HAp scaffolds. *Journal of the Mechanical Behavior of Biomedical Materials,* 2020, **104**, 1–7, doi: 10.1016/j.jmbbm.2020.103616.

8. WACH, Radoslaw A., WOLSZCZAK, Piotr, ADAMUS-WLODARCZYK, Agnieszka. Enhancement of mechanical properties of FDM-PLA parts via thermal annealing. *Macromolecular Materials and Engineering,* 2018, **303**(9), 1–9, doi: 10.1002/mame.201800169.
9. CHALGHAM, Ali, WICKENKAMP, Inge, EHRMANN, Andrea. Mechanical properties of FDM printed PLA parts before and after thermal treatment. *Polymers,* 2021, **13**(8), 1–10, doi: 10.3390/polym13081239.
10. AMBONE, Tushar, TORRIS, Arun, SHANMUGANATHAN, Kadhiravan. Enhancing the mechanical properties of 3D printed polylactic acid using nanocellulose. *Polymer Engineering and Science,* 2020, **60**(8), 1842–1855, doi: 10.1002/pen.25421.
11. DOU, Hao, CHENG, Yunyong, YE, Wenguang, ZHANG, Dinghua, LI, Junjie, MIAO, Zhoujun, RUDYKH, Stephan. Effect of process parameters on tensile mechanical properties of 3D printing continuous carbon fiber-reinforced PLA composites. *Materials* 2020, **13**(17), 1–15, doi: 10.3390/ma13173850.
12. KAMAAL, M., ANAS, M., RASTOGI, H., BHARDWAJ, N., RAHAMAN, A. Effect of FDM process parameters on mechanical properties of 3D-printed carbon fibre–PLA composite. *Progress in Additive Manufacturing,* 2021, **6**, 63–69, doi: 10.1007/s40964-020-00145-3.
13. WANG, Shuheng, MA, Yongbin, DENG, Zichen, ZHANG, Sen, CAI, Jiaxin. Effects of fused deposition modeling process parameters on tensile, dynamic mechanical properties of 3D printed polylactic acid materials. *Polymer Testing,* 2020, **86**, 1–8, doi: 10.1016/j.polymertesting.2020.106483.
14. GORLACHOVA, Maryna, MAHLTIG, Boris. 3D-printing on textiles – an investigation on adhesion properties of the produced composite materials. *Journal of Polymer Research,* 2021, **28**, 1–10, doi: 10.1007/s10965-021-02567-1.
15. POPESCU, Diana, and AMZA, Catalin Gheorghe. 3D printing onto textiles: a systematic analysis of the adhesion studies. *3D Printing and Additive Manufacturing* 2024, **11**(2), e586–e606, doi: 10.1089/3dp.2022.0100.
16. KOČEVAR, Tanja Nuša. 3D printing on textiles – overview of research on adhesion to woven fabrics. *Tekstilec,* 2023, **66**(3), 164–177, doi: 10.14502/tekstilec.66.2023055.
17. MPOFU, Nonsikelelo Sheron, MWASIAGI, Josphat Igadwa, NKIWANE, Londiwe Cynthia, GITHINJI, David Njuguna. The use of statistical techniques to study the machine parameters affecting the properties of 3D printed cotton/polylactic acid fabrics. *Journal of Engineered Fibers and Fabrics,* 2020, **15**, 1–10, doi: 10.1177/1558925020928531.
18. ČUK, Marjeta, BIZJAK, Matejka, KOČEVAR, Tanja Nusa. Influence of simple and double-weave structures on the adhesive properties of 3D printed fabrics. *Polymers,* 2022, **14**(14), 1–18, doi: 10.3390/polym14040755.
19. ČUK, Marjeta, BIZJAK, Matejka, MUCK, Deja, KOČEVAR, Tanja Nuša. 3D printing and functionalization of textiles. In *10th International Symposium on Graphic Engineering and Design*, 2020, 499–506, doi: 10.24867/GRID-2020-p56.
20. MPOFU, Nonsikelelo Sheron, MWASIAGI, Josphat Igadwa, NKIWANE, Londiwe C., NJUGUNA, David. Use of regression to study the effect of fabric parameters on the adhesion of 3D printed PLA polymer onto woven fabrics. *Fashion and Textiles,* 2019, **6**, 1–12, doi: 10.1186/s40691-019-0180-6.
21. GÖRMER, Daniel, STÖRMER, Jannik, EHRMANN, Andrea. The influence of thermal after-treatment on the adhesion of 3D prints on textile fabrics. *Communications in Development and Assembling of Textile Products,* 2020, **1**(2), 104–110, doi: 10.25367/cdatp.2020.1.p104-110.
22. KOZIOR, Tomasz, DÖPKE, Christoph, GRIMMELSMANN, Nils, JUHÁSZ JUNGER,

Irén, EHRMANN, Andrea. Influence of fabric pretreatment on adhesion of three-dimensional printed material on textile substrates. *Advances in Mechanical Engineering* 2018, **10**(8), 1–8, doi: 10.1177/1687814018792316.

23. KORGER, Michael, GLOGOWSKY, Alexandra, SANDULOFF, Silke, STEINEM, Christine, HUYSMAN, Sofie, HORN, Bettina, ERNST, Michael, RABE, Maike. Testing thermoplastic elastomers selected as flexible three-dimensional printing materials for functional garment and technical textile applications. *Journal of Engineered Fibers and Fabrics,* 2020, **15**, 1–10, doi: 10.1177/1558925020924599.
24. SITOTAW, Dereje B., MUENKS, Dominik, KYOSEV, Yordan, KABISH, Abera K. Influence of fluorocarbon treatment on the adhesion of material extrusion 3D prints on textile. *Journal of Industrial Textiles,* 2022, **52**, 1–14, doi: 10.1177/15280837221137014.
25. BLAIS, Maxwell, TOMLINSON, Scott, KHODA, Bashir. Investigation of the Interfacial Adhesion Strength of Parts Additively Manufactured on Fabrics. *ASME Open Journal of Engineering,* 2023, **2**, 1–6, doi: 10.1115/1.4062281.
26. KEEFE, Edmund M., THOMAS, Jack A., BULLER, Gary A., BANKS, Craig E. Textile additive manufacturing: an overview. *Cogent Engineering,* 2022, **9**(1), 1–17, doi: 10.1080/23311916.2022.2048439.
27. GROTHE, Timo, BROCKHAGEN, Bennet, STORCK, Jan Lukas. Three-dimensional printing resin on different textile substrates using stereolithography: a proof of concept. *Journal of Engineered Fibers and Fabrics,* 2020, **15**, 1–7, doi: 10.1177/1558925020933440.
28. KOZIOR, Tomasz, EHRMANN, Andrea. First proof-of-principle of PolyJet 3D printing on textile fabrics. *Polymers,* 2023, **15**(17), 1–9, doi: 10.3390/polym15173536.
29. BOCHNIA, Jerzy, KOZIOR, Tomasz, SZOT, Wiktor, RUDNIK Mateusz, ZMARZLY, Pawel, GOGOLEWSKI, Damian, SZCZYGIEL, Pawel, MUSIALEK, Mateusz. Selected mechanical and rheological properties of medical resin MED610 in PolyJet matrix three-dimensional printing technology in quality aspects. *3D Printing and Additive Manufacturing,* 2024, **11**(1), 299–313, doi: 10.1089/3dp.2022.0215.
30. KORGER, M., BERGSCHNEIDER, J., LUTZ, M., MAHLTIG, B., FINSTERBUSCH, K., RABE, M. Possible applications of 3D printing technology on textile substrates. *IOP Conference Series: Materials Science Engineering* 2016, **141**, 1–6, doi: 10.1088/1757-899X/141/1/012011.
31. EVANS, Nathan T., IRVIN, Cameron W., SAFRANSKI, David L., GALL, Ken. Impact of surface porosity and topography on the mechanical behavior of high strength biomedical polymers. *Journal of the Mechanical Behavior of Biomedical Materials,* 2016, **59**, 459–473, doi: 10.1016/j.jmbbm.2016.02.033.
32. TORSTRICK, F. Brennan, EVANS, Nathan T., STEVENS, Hazel Y., GALL, Ken, GULDBERG, Robert E. Do surface porosity and pore size influence mechanical properties and cellular response to PEEK? *Clinical Orthopaedics and Related Research,* 2016, **474**, 2373–2383, doi: 10.1007/s11999-016-4833-0.
33. CALORE, Andrea Roberto, SRINIVAS, Varun, GROENENDIJK, Linda, SERAFIM, Andrada, STANCU, Izabela Cristina, WILBERS, Arnold, LEONÉ, Nils, ALBILLOS SANCHEZ, Ane, AUHL, Dietmar, MOTA, Carlos, BERNAERTS, Katrien, HARINGS, Jules A. W., MORONI, Lorenzo. Manufacturing of scaffolds with interconnected internal open porosity and surface roughness. *Acta Biomaterialia,* 2023, **156**, 158–176, doi: 10.1016/j.actbio.2022.07.017.
34. TUVSHINBAYAR, Khorolsuren, MPOFU, Nonsikelelo Sheron, BERGER, Thomas, STORCK, Jan Lukas, BÜSGEN, Alexander, EHRMANN, Andrea. Comparison of FDM and SLA printing on woven fabrics. *Communications in Development and Assembling of Textile Products*, in print.

35. Dental materials [online]. STRATASYS [accessed 26. 6. 2024]. Available on World Wide Web: <https://www.stratasys.com/siteassets/3d-printers/printer-catalog/polyjet/j700-dental-printer/dental-3d-printing-materials-data-sheet.pdf>.

36. Biocompatible Clear MED610 [online]. STRATASYS [accessed 26. 6. 2024]. Available on World Wide Web: <https://www.stratasys.com/siteassets/materials/materials-catalog/biocompatible/mds_pj_med610_0720a.pdf?v=48e364>.

Appendix

CLSM images taken at three positions (P1, P2, P3) of three samples (S1, S2, S3) per material combination

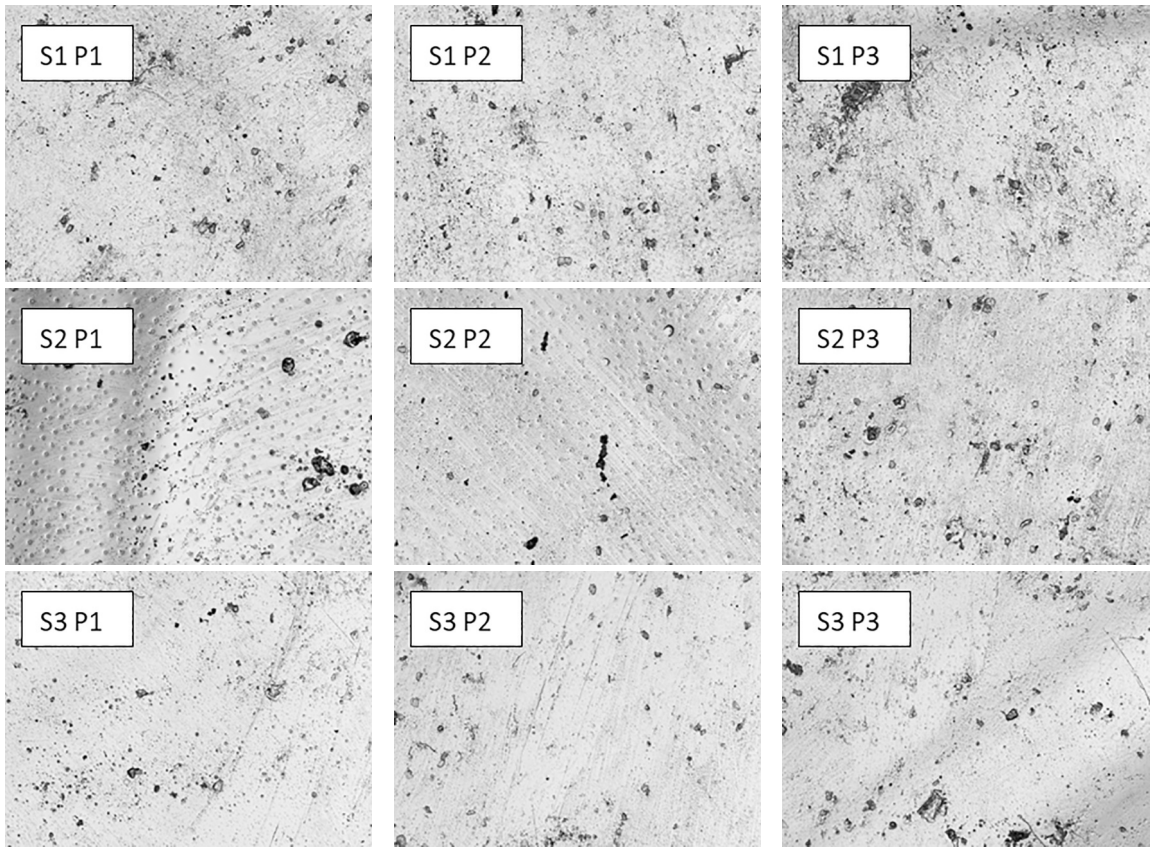

Figure A1: CLSM images on pure MED610 samples. Images sizes correspond to 1.4 mm x 1.05 mm.

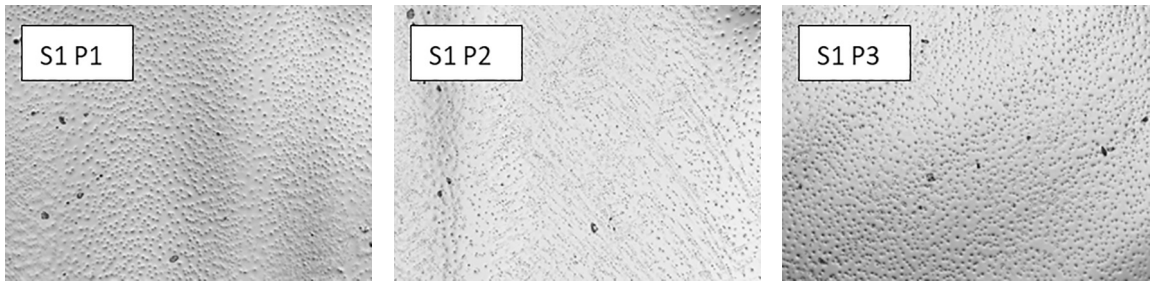

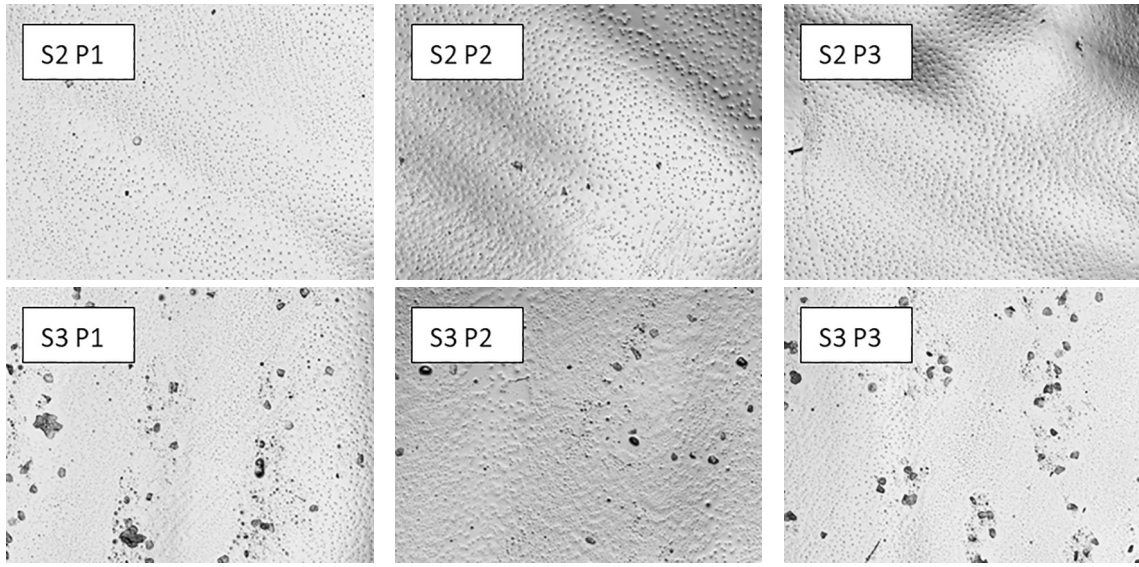

Figure A2: CLSM images on MED610 on cotton. Images sizes correspond to 1.4 mm x 1.05 mm.

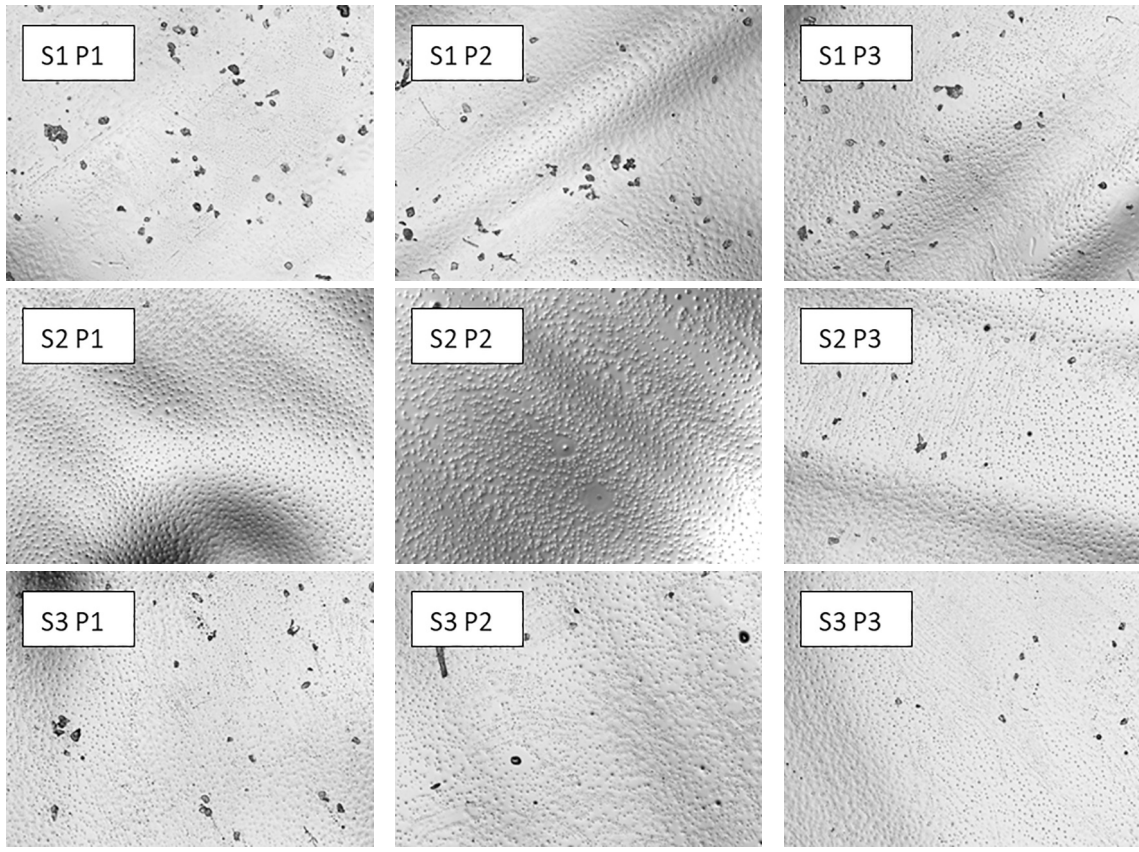

Figure A3: CLSM images on MED610 on linen. Images sizes correspond to 1.4 mm x 1.05 mm.

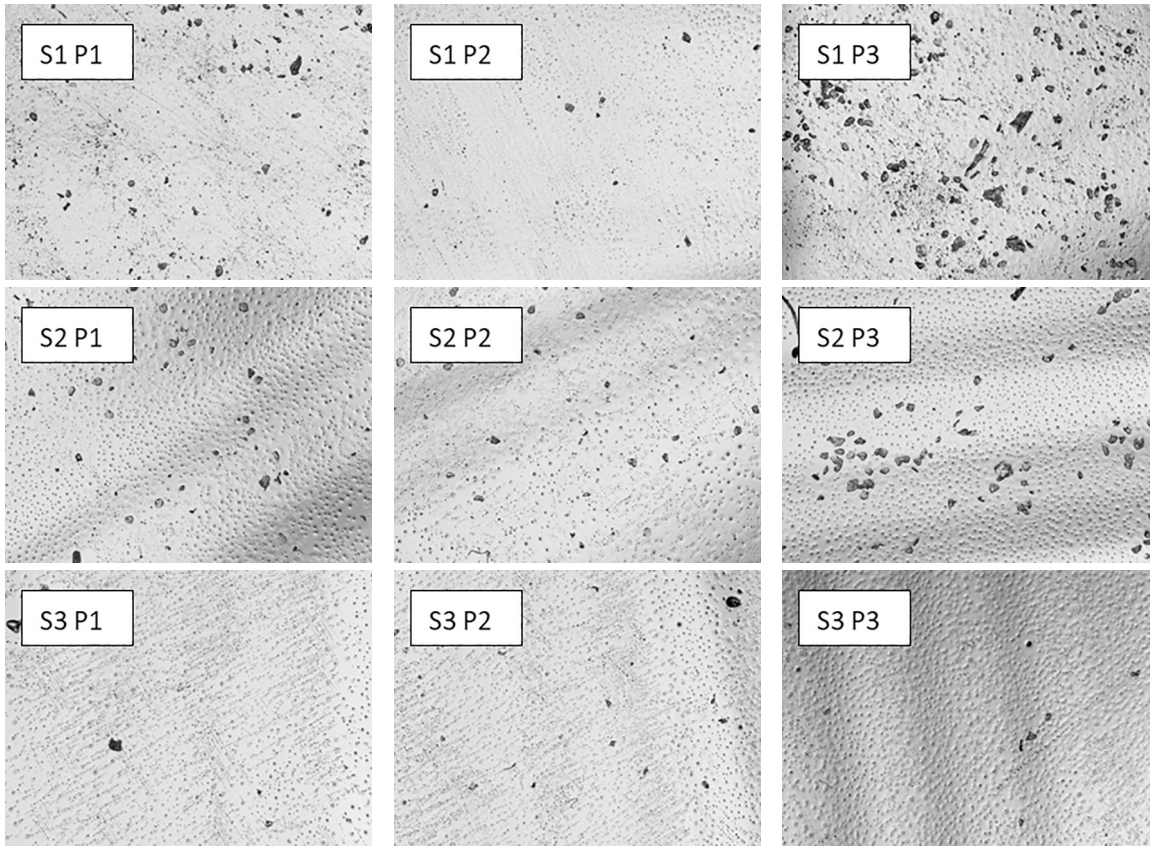

Figure A4: CLSM images on MED610 on polyester "micropeach". Images sizes correspond to 1.4 mm x 1.05 mm.